Journal of Geomatics Science and Technology

Real-Time Kinematic Network of Tehran, from Design to Application

M. Mashhadi-Hossainali*[1], M. Khoshmanesh [2]

[1]Associate Professor, Department of Geodesy and Geomatics Engineering, K. N. Toosi University of Technology, Tehran, Iran.
hossainali@kntu.ac.ir

[2]PhD Candidate, School of Earth and Space Exploration, Arizona State University, Tempe, AZ, USA.
mostafa_khoshmanesh@yahoo.com

(Received: September 2014, Accepted: August 2016)

Key Words: Real Time Positioning, Global Navigation Satellite Systems, Network Design

Abstract

Following the request of the Tehran municipality and in order to provide the spatial information required in their various projects, a real-time kinematic network has been designed for Tehran. Based on the existing measures such as the dilution of precision at the network point positions, two different designs have been proposed. A minimum number of six GNSS stations are used in both of the proposed designs. In contrary to the first design (Design 1), the second design (Design 2) provides a better coverage within the city. The impact of the distance dependent errors within the proposed designs as well as the other existing measures has been analyzed for selecting the optimum design. The GNSS almanac as well as the IGS GIM and meteorological data obtained from the existing synoptic stations within and next to the city are used for this purpose. Totally, only the effect of tropospheric refraction suggests the second design as the optimum one in this project. GNSS measurements made at this network point positions are used to verify the measures used through the design process. Two testing approaches have been used to check the efficiency of the designed network in real-time applications. In the first approach and within the city of Tehran point positions are determined independently using kinematic as well as static positioning techniques. Different correction estimation and dissemination algorithms including FKP, MAX and i-MAX techniques have been applied for this purpose. In the second approach, the central and northern reference stations of the network, separately plays the role of a rover receiver (test point) while it is not contributing in computing the network corrections. Repeatability, accuracy and precision of these points' positions have been analyzed. Result of this verification analysis acknowledges the applied method to design the TNRTK. Accuracy of 1 to 3 cm is achieved in the coordinate components within the network area. However, the accuracy of the point positions outside of the network area, especially height components, is not fulfilling the presupposed accuracy of an NRTK due to the tropospheric effects.

* Corresponding Author

1. Introduction

Real time kinematic positioning (RTK) is a differential positioning technique. In this method, accuracy of a few centimeters for the coordinates of a roving receiver is achieved by resolving the ambiguity of the phase observations and reducing the distance dependent errors between a reference and a rover receiver. This is done by modeling the errors as well as the transmission of the corresponding corrections to the roving receiver.

The reference receiver is installed on a fixed or known station. Coordinates of the fixed or reference receiver is used for resolving the ambiguity of the simultaneous phase observations made at the fixed and rover receivers. The obtained accuracy highly depends on the existing correlation between the positioning signals received at the reference and roving receivers. This usually restricts the inter receivers distance to 10km or less (Rizos, 2003). As the result, the efficiency of the method decreases by increasing the distance between the reference and rover receivers.

An RTK positioning network (NRTK) consists of several reference stations which continuously measure the code and phase pseudo-ranges to the GNSS satellites. Simultaneous measurements of the network stations are used for modeling the errors. Therefore, estimated corrections are valid within the network area (Wübbena et al. 1996, Han 1997). In contrary to the traditional RTK positioning, if some of the reference stations failed to operate; the network would still provide the required corrections to users using the rest of the stations. An NRTK user is able to determine his position with an accuracy of 2 to 3 cm in horizontal and 3 to 5 centimeters in the vertical component within the network area. Moreover, the positioning accuracy of a rover is more homogeneous in an RTK network as compared to the traditional (single base) RTK.

Different methods have been proposed for estimating the corrections used for reducing distance-dependent biases in RTK networks. Due to the fact that each technique can obtain a special level of accuracy, the differences between these methods have to be taken under cautious attention in design and implementation of an RTK network (see, e.g. Landau et al. 2003 and Janssen 2009). In any way, in an ideal RTK network any of these techniques is applicable.

To date, several regional RTK networks are operational worldwide: Chen et al (2000) reports on the design of the Singapore Integrated Multiple Reference Station Network. A method based on Kalman filter is used for resolving the carrier phase ambiguities in this NRTK. Moreover, the linear combination method proposed by Han (1997) has been adopted in order to generate the network corrections. Using the same method for resolving ambiguities and implementing the method of Virtual Reference Station (VRS), Rizos and Yan (2004) have designed the Sydney RTK Network (SydNet). Gordini et al. (2006) describes the Victoria Continuously Operating Reference Station (CORS) network, established in Australia, the adopted procedures in evaluating the performance of the network and the obtained practical results. The quality of VRS was also studied in the conditions that are typical in Finland and northern latitudes by Hakli (2004). Using the method of VRS for generating the corrections, centimeter level accuracy has been attained in this NTRK if in an obstacle free horizon a minimum of 5 common satellites are tracked and a maximum GDOP value of 8 is attained. Another important outcome of this study is the homogeneity of the RTK solutions' accuracy within the network area. This is due to the existing low correlation between the accuracy of the RTK solution and the distance between a rover and the nearest reference station in an NRTK. Additionally, Vollath et al. (2002) explain the reduction of initialization times, improvement in position accuracy and increase in reliability seen in network RTK systems. RTK networks in the Netherlands (Marel, 1998), Japan (Petrovski et al. 2002,), and Arab Emirates (El-Mowafy et al. 2003) are also other examples of victorious RTK network design worldwide.

Following the request of the Tehran municipality and in order to provide the spatial information required in the various running and planned projects of the city as well as the continuing progress in public demand for real time spatial information such as mobile mapping, cadastral surveying, etc; a real-time kinematic network has been designed for Tehran. This paper reports on the adopted methods for designing, realization and testing of the Tehran RTK network (TNRTK).

TNRTK hardware and software infrastructure supports all the existing methods for estimating and transmission of the distance-dependent errors. The quality measures used for this purpose are practically analyzed using the GNSS data of a 24 hour campaign. A set of test points has been used to check the efficiency of this network in RTK positioning within the city. Statistical methods are the mathematical apparatus used for this purpose. Section 2 of this paper discusses on the process which resulted in this network design. The third section reports on the evaluation of the quality measures used in choosing the optimum design. The Fourth section presents the adopted methodology for testing the TNRTK and the corresponding obtained results. Finally, the efficiency of the proposed design is assessed in the concluding section of the paper (section 5).

2. Designing the RTK Network of Tehran

The promised precision of an RTK network demands a comprehensive consideration of the network design. Designing an RTK network is a more challenging problem compared to a GNSS network due to more involved parameters. This is not only due to the small positioning time required for an RTK solution but also the impact of distance-dependent errors on the rover coordinates. The small time interval involved in RTK positioning reduces the redundancy of measurements. This can be partially compensated by using a proper network design: reducing the extent of an RTK network increases the visibility of the GNSS satellites between both RTK reference and rover receivers. On the other hand, the impact of distance-dependent errors increases with the distance between a rover and the network reference stations. Therefore, the RTK network size should be large enough in order that the network corrections could cover the spatial variations of the errors within the area in which the NRTK service is supposed to be available. Based on the discussion above, two different designs can be proposed for the TNRTK. Figures (1a) and (1b) illustrate the proposed designs. By using one central station in the network design, the distances between NRTK users to at least three reference stations are minimized. This is why a central point is seen in both of the two proposed designs.

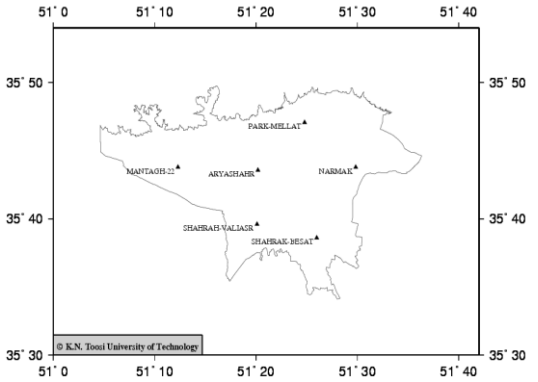

(a)

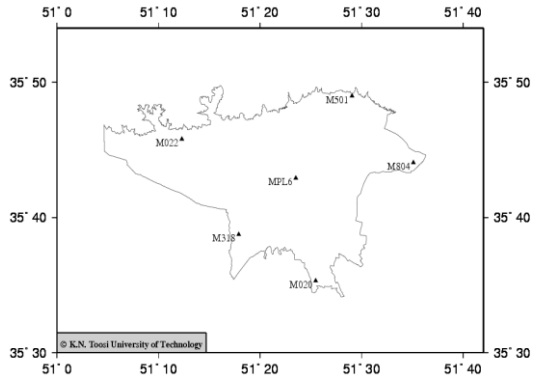

(b)

Fig. 1: The two proposed designs for the Real Time Kinematic Network of Tehran: (a) Design No. 1 & (b) Design No. 2

To analyze the efficiency of the proposed designs a comprehensive set of measures has been taken into account. These include the pre-analysis of the general measures which are usually considered in planning a satellite geodetic network as well as the impact of distance-dependent errors on the network size and the distribution of the points.

2.1. General measures in an RTK network design

A number of general measures are usually used in planning a GNSS survey in geodesy. These include the analysis of the visibility of the GNSS satellites, the geometry of positioning, the elevation angle of the visible satellites and the signal to noise ratio. It is customary to use commercial packages, known as planning software, for this purpose. In these packages, for a couple of base stations (in network mode) the planning measures are simply the mean of their estimates for every station of the network. To avoid the simplified algorithms used in these packages, the design measures are computed using K. N. Toosi Planning software (KNTP) (Mehrabadi, 2012).

This software implements simulated doubly-differenced phase and code measurements for this purpose. Sky visibility at each station and the GNSS almanac are the required inputs in this process.

Since the reference stations of an RTK network should be connected to the network server via a high speed communication link, the reference stations are supposed to be located in the headquarters of municipality located at six districts of the city. The headquarters of the city districts in Tehran are connected via optical fibers. This link supports fast transmission of the GNSS measurements to the network server for computing the corrections.

2.1.1. Number of common visible satellites

The number of satellites simultaneously tracked from the network reference and roving receivers is a prominent parameter in an RTK network design. This is due to the limited time available for resolving the carrier phase ambiguities in the real time positioning process. Decreasing the network size increases the number of satellites commonly tracked from the network reference and roving receivers. This increases the redundancy of measurements as well as the success rate in resolving the ambiguity of carrier phase observations at the roving receivers. As the result, the coordinates of a rover is estimated more rapidly with a higher precision. KNTP software is used to come up with an idea about the visibility of the satellites (see Figure 2). Additionally, Table 1 and Table 2 compare the time to fix of various baselines between a rover and the network reference stations in the two proposed designs. The central point in each design is taken as the position for the roving receiver.

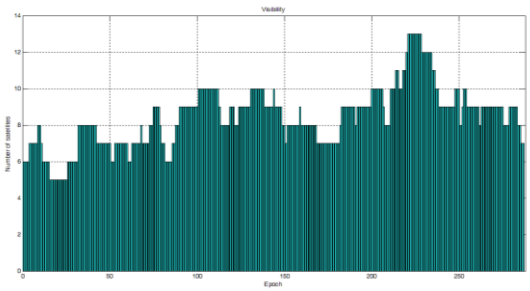

(a)

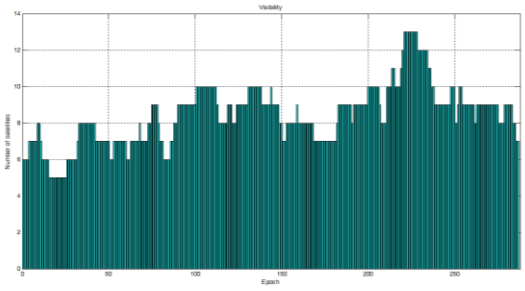

(b)

Fig. 2: Number of satellites tracked form the TNRTK reference stations: (a) Design No. 1& (b) Design No. 2

Table 1: Time to fix for the baselines between the TNRTK reference stations and a rover located at the network's central point – Design No. 1

Baseline Length [km]	Time to fix ($L1$) [epochs]	Time to fix ($L2$) [epochs]
7.33798	20	10
11.8998	26	18
9.50581	22	14
12.7103	27	19
14.5609	29	19

Table 2: Time to fix for the baselines between the TNRTK reference stations and a rover located at the network's central point – Design No. 2

Baseline Length [km]	Time to fix ($L1$) [epochs]	Time to fix ($L2$) [epochs]
14.3684	30	20
17.7355	35	21
11.4566	25	17
13.9892	29	20
17.6258	35	21

According to Fig. 2, the visibility of the GNSS satellites are almost the same for both of the proposed designs. On the other hand, the smaller amounts of time to fix estimated for the first design is due to smaller baseline lengths involved in this design. Nevertheless, for normal applications such as cadastral surveying there is no remarkable difference between the two proposed designs in this particular point of view.

2.1.2. Geometry of positioning

The precision of a point position is not only controlled by the noise of the phase and code measurements, but also with the relative position of the GNSS satellites and the network stations or the geometry of positioning. The role of this measure is more crucial in kinematic positioning as compared to positioning in static mode. This is because, by

increasing the observation time (in static positioning) a variety of geometries are involved in the positioning process. The geometry of positioning is formulated through the Position Dilution of Precision (PDOP) defined as follows:

$$PDOP = \sqrt{trace\left(\mathbf{A}^T\mathbf{A}\right)^{-1}} \quad (1a)$$

$$\mathbf{A}_{AB}^{kl}(i,:) = \left[\frac{\partial \rho_{AB}^{kl}}{\partial x_B} \quad \frac{\partial \rho_{AB}^{kl}}{\partial y_B} \quad \frac{\partial \rho_{AB}^{kl}}{\partial z_B} \quad 0 \quad 0 \quad -\lambda \right] \quad (1b)$$

In which $\mathbf{A}$ is the design matrix. The i[th] row of this matrix is given by Eq. (1b) for carrier phase measurements. In this equation ρ_{AB}^{kl} is the doubly-differenced geometric distance of reference station A and roving receiver B to satellites k & l and λ is the wavelength of the carrier signal (Blewitt G. 1998). The impact of positioning geometry on the TNRTK coordinates is almost the same for the two proposed designs. Therefore, this general measure does not play any role in choosing the optimum network designs.

2.1.3. Elevation angle of detected satellites

Pseudo-ranges measured to low elevation satellites are more biased than pseudo-ranges made to the high elevation ones. Moreover, biased measurements can prevent the successful resolution of initial phase ambiguities. Consequently, elevation angle of the GNSS satellites is another key measure which has to be considered in the network design. KNTP is used for computing and illustrating the elevation angles of the GPS satellites for both of the proposed design.

The majority of the satellites are expected to be tracked above the elevation mask of 20 degrees. Moreover, from this point of view there is no remarkable difference between the two proposed designs. Thereof, the possibilities of failure in resolving the ambiguity of long baselines are the same for both of the proposed plans.

2.1.4. Noise of measurement environment

Radio signal transmitters nearby a GNSS receiver may increase the noise of the GNSS satellites' signals. Reducing the signal to noise ratio (signal strength) decreases the success rate in ambiguity resolution. On the other hand, resolution of the initial phase ambiguities is crucial for real time kinematic positioning of a moving receiver. Therefore, the signal to noise ratio should be large enough at position of both RTK reference and rover receivers. Evaluation of this measure demands measurement at the proposed positions for the reference stations of an RTK network. The threshold value of 40 decibel has been suggested and adopted for this purpose. The corresponding results are given in the next section of the paper.

2.2. Special measures in an RTK network design

The functionality of an RTK network depends on the efficiency of the corrections computed for the distance-dependent errors in the network area. The corrections are computed from the measurements of the network reference stations. Variations of these errors, therefore, play a key role in selecting the optimum position for the permanent stations of an RTK network. The geometric approach developed by Beutler et al. (1988) is used for analyzing the errors' variation within the study area.

2.2.1. Orbit error

Before the public release of the IGS orbital products, the orbit quality was considered as one of the primary accuracy limiting factors in the applications of the GNSS systems in geodesy. Bauersima (1983) gives a handy rule of thumb for analyzing the impact of the orbital errors in the baseline components:

$$\Delta x(m) \approx \frac{l}{d}\Delta X(m) \quad (2)$$

In this equation, l is the baseline length, $d \approx 25000\,Km$ is the approximate distance between the satellite system and the survey area, ΔX is the orbital error and Δx is the impact of orbital error on the baseline components. This equation gives satisfactory results for measurement sessions of about 1-2 hours or less. Zielinski (1988) gives a new formula which is more optimistic by a factor of 4-10 in horizontal components and a factor of 1 for the vertical component in permanent measurements. Since in the design step the

expected accuracy of the horizontal and vertical components of the point coordinates are the same, Eq. (2) is more appropriate for analyzing the impact of orbital errors on the size of an NRTK.

Today, broadcasted ephemerides are the most accurate real time orbits. The accuracy of this orbital product is considered to be better than 260 centimeters (Seeber, 2003). On the other hand, the biggest baselines in each of the two proposed designs are 26.5 and 34.5 kilometers respectively. Considering the expected sub-centimeter accuracy in estimating the reference stations' coordinates as well as the corresponding errors forecasted by Eq. (2) for the baseline components, this orbital error results in the coordinate components whose accuracy is better than the expected operational accuracy of TNRTK (1-3 centimeters) for a roving receiver in both proposed designs.

2.2.2. Electron density variation in Ionosphere layer

Since deactivation of Selective Availability (SA), the refraction of the GNSS electromagnetic waves in Ionosphere layer dominates the accuracy of positioning using single frequency receivers (see e.g. Klobuchar, 1987). To the first order of approximation, the magnitude of this error is given by:

$$d\rho = \pm \frac{a}{f^2 \cos z'} TEC \qquad (3)$$

Where $d\rho$ is the corresponding bias in the satellite-receiver distance. This bias is positive in positioning with carrier phase measurements and is negative in positioning with code pseudo-ranges. Moreover, $a = 4.03 \times 10^{17}\, ms^{-2} TECU^{-1}$ is a constant, f is the frequency of the carrier wave, z' is zenith distance of the satellite at the ionospheric pierce point, and TEC or Total Electron Content is the linear integral of the electron density along the propagation path of the carrier signal from GNSS satellites to a receiver. TEC is normally developed into a series of base functions on the surface of a reference layer. The height of this layer is usually set to the height of the maximum electron density obtained from the Chapman profile (see e.g. Feltens 1998). Spherical harmonics and polynomials are used as the base functions in global/regional and local extents respectively (Schaer et al. 1995, Wild et al. 1989).

Assuming a symmetric distribution of the GNSS satellites in view, ionospheric bias $d\rho$ produces the following scale error (Beutler at al., 1988) in the network solution:

$$\frac{\Delta l}{l} = -\frac{a}{R.f^2 \cos z_{\max}} TEC \qquad (4)$$

In this equation $z_{\max}$ is the maximum zenith angle of the GNSS satellites in view and R is the mean radius of the earth. Using $z_{\max} = 70^\circ$, $f_1 = 1.57542 \times 10^9\, Hz$ and the values of $TEC_{\min} = 0.5 \times 10^{17}\, TECU$ and $TEC_{\max} = 5 \times 10^{17}\, TECU$ which are expected to occur at midnight and noon time respectively, the corresponding scale error would range from $-0.35\, ppm$ to $-3.5\, ppm$. At least for small areas, the horizontal gradient of TEC is expected to be less than the temporal range above. Nevertheless, to select an optimum extent for an RTK network that guarantees the expected real time accuracies of 1 to 3 centimeters, having a-priori information on horizontal variations of TEC is necessary. Therefore, the IGS TEC maps have been used for analyzing the horizontal variations of TEC within the study area. VTECs have been interpolated using the method of Smith and Wessel (1990). According to the obtained results, the maximum horizontal gradient of TEC is expected to be about $0.014\, TECU/Km$ in Tehran. This gradient predicts TEC difference of $0.126 TECU$ between station "PARK-MELLAT" of the first proposed design and the northernmost part of Tehran city. Using Eq. (4) with the input constants given before, this difference in TEC results in the scale error of about $-0.01 ppm$. Thereof, considering the required accuracies in the TNRTK, the impact of this bias does not impose any constraint on the size or extent of this RTK network.

2.2.3. Tropospheric variation

Refraction index for the GNSS signals in troposphere is a function of temperature, pressure and humidity. The tropospheric path delay is normally separated into dry and wet components. Although the path delay originating from the wet component shows a much higher variability compared to the dry

part, its contribution is only 10% of the total delay (Leick 1994). Therefore, to decide on the appropriate network design for the RTK network of Tehran, the contribution of the dry part has been taken into account.

Assuming a symmetric distribution of the GNSS satellites in view, Beutler et al. (1988) investigated the impact of this error on the network coordinates. According to this study: assuming maximum zenith angle of $z_{\max} = 70^{o}$ for the satellites in view, neglecting the refraction of the GNSS signals in this layer of atmosphere produces a scale error of $0.4\,ppm$. Moreover, sensitivity analysis of the Saastamoinen's model for the dry part of tropospheric delay, given in Table 3, indicates that 1 degree of centigrade error in measuring temperature at one end of a baseline produces 27 mm bias in the estimated height of the other end. The corresponding bias for the measurement errors of the other parameters are also given in this table.

Table 3: Sensitivity analysis of the Saastamonin's model for the tropospheric dry path delay, after Beutler et al., (1988)

Atmospheric condition			Gradiant of the tropospheric slant delay		
$T(^{0}C)$	$P(mbar)$	H (%)	$\left\|\frac{\partial r}{\partial T}\right\| mm/^{0}C$	$\left\|\frac{\partial r}{\partial p}\right\| mm/mbar$	$\frac{\partial r}{\partial H} mm/1\%$
0^{0}	1000	100	5	2	0.6
30^{0}	1000	100	27	2	4.0
0^{0}	1000	50	3	2	0.6
30	1000	50	14	2	4.0

Differences of temperature, humidity and pressure between the network stations in the first proposed design and points at the outermost part of the city (station "PARK-MELLAT" in this design and the northern most part of the city for example) can be treated as the corresponding measurement errors when the correction for the tropospheric delay is to be computed using the simultaneous phase and code measurements of the first design. Considering the west-east direction of wind within the city of Tehran and the large height differences between the northern and southern parts of the city as well as the remarkable magnitude of the biases produced by the tropospheric delay, to decide on the appropriate network design further analysis of this source of error is necessary. For this purpose, temperature, pressure and humidity records of four synoptic stations nearby the city have been used. Figure 5 illustrates the position of the synoptic stations used in this study. Figure 6 gives for example the monthly averages of temperature at the 4 stations above during the year 2005.

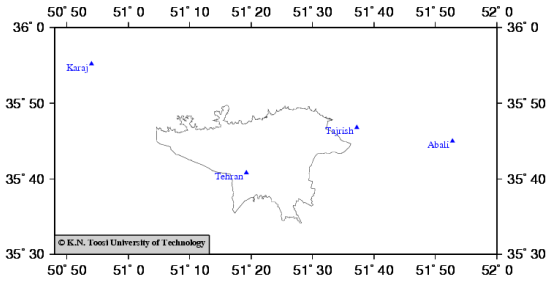

Fig. 5: Spatial distribution of the synoptic stations in this study

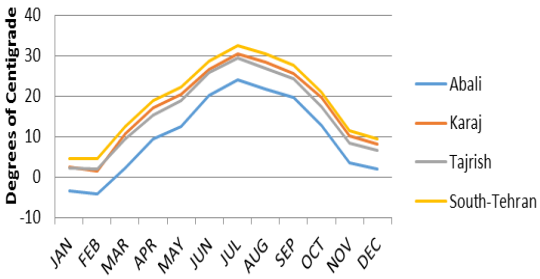

Fig. 6: Monthly average of surface temperature of four synoptic meteorological stations nearby to the city of Tehran

The average monthly variation of temperature in the north-south direction of the city is more than 5 degrees of centigrade. Assuming a linear trend for the gradient of temperature between the northern and southern parts of the city, temperature gradient in this direction is $0.38^{\circ}C/km$. This gradient predicts 4 degrees of centigrade change in the temperature at the position of station "PARK-MELLAT" in the first design and the northernmost point of the city. This temperature change produces a bias which is more than the expected accuracies of TNRTK. As the result, in order to assure the expected accuracies in real time kinematic network of Tehran, application of the second design is inevitable.

3. Evaluation of Design Measures

After selecting the optimum design for the TNRTK, the communication infrastructure of the network and the reference stations have been set up. All the reference stations are connected to a server. The data transferred from reference stations is managed by the Leica Spider software package. Twenty four hours of simultaneous code and carrier phase

measurements of the reference stations have been used to check the measures involved in selecting the optimum design. This section reports the corresponding results.

3.1. Implemented Hardware in Tehran RTK Network

The 120 channel GRX1200+GNSS receivers and Leica AS10 antenna have been used in the TNRTK. This type of receiver is able to receive L1, L2 and L5 signals from GPS system. Leica AS10 is a water-proof antenna and can be used in temperature range of -40 to 70 degrees of centigrade. Observations of the reference stations are mustered by a central server and are processed using the GNSS Spider software mentioned above. The Spider software manages the network corrections in three different formats: iMAX in RTCM v2.3, MAX in RTCM v3.0, and FKP.

3.2. Evaluation of the general design measures

3.2.1. Satellite visibility

Considering the size of the TNRTK, simultaneous detection of all the satellites in view is anticipated within the expected service domain for this NRTK. To verify this argument the number of GPS and GLONASS satellites in view at the reference points of the network has been surveyed using the 24 hour session of continuous measurements. The results reveal that 53 GNSS satellites are visible from all the stations of the chosen design during a complete day. These consist of 31 GPS satellites (G2 to G32) and all the GLONASS satellites except R3 and R4. On the other hand, investigation of the detected GPS and GLONASS satellites for the longest baseline of the network (i.e. stations M804 and M022) shows almost a complete overlap for these two stations.

3.2.2. Elevation Angle of the GNSS Satellites

Analyzing the visibility of the GNSS satellites and their elevation angle provide a measure to evaluate the sky view at the position of the reference stations. The ratio of the number of observations above a specific elevation angle to the number of observations above the horizon (at each station) can be taken as a quantitative parameter for this purpose. The number of observations in horizon is computed using the expected positions of the GNSS satellites obtained from the navigation files. This ratio is computed for all of the detected GPS and GLONASS satellites. This analysis illustrates that at least 81.72% of measurements are made above the elevation mask of 10 degrees. This ratio increases to 87.17% for the point which is located at the northernmost part of the city. The slight change of this ratio exhibits a fairly equal condition for the network stations in this particular point of view.

3.2.3. Positioning Geometry

For the optimum design, the expected maximum PDOP has been predicted to reach 2.63 when GPS and GLONASS satellites are taken into account. To check this measure in practice, the average, minimum, and maximum PDOP values has been calculated for the measurements of the session in question. Table 4 reports on the obtained results. Reported PDOPs are computed in single station (absolute positioning) mode.

The comparison of expected PDOPs in single station mode computed using commercial software for planning to that of the network (relative positioning) mode computed using KNTP shows that the predicted PDOP in the later mode is almost half of its value in single station mode. Thereof, the maximum PDOP of the network would be less than about 2.5 in practice. Considering 2mm accuracy for phase observations, this threshold for the spatial geometry of satellites in view results in sub-centimeter impact in the accuracy of positioning for the reference stations.

Table 4: Computed PDOPs using GNSS measurements and commercial software

Marker Name/Number	Min PDOP	Max PDOP	Ave PDOP
Region1/M501	2.2	5.2	2.9
Region4/M804	2.2	4.5	2.8
Region6/MPL6	2.2	4.5	2.8
Region18/M318	2.2	4.5	2.8
Region20/M020	2.3	4.5	2.8
Region22/M022	2.2	4.6	2.8

3.2.4. Noise of measurements

The evaluation of the signal to noise ratio stipulates the analysis of the data measured in the aforementioned campaign. The 24 hour averaged signal to noise ratios estimated using the program TEQC (Estry and Meertens 1999)

for GPS and GLONASS observations at each of the reference points are given in Table 5.

Table 5: Average signal to noise ratio for the reference stations of TNRTK

	GPS		GLONASS	
Marker Name/Number	L1	L2	L1	L2
Region1/M501	47.7	42.3	46.7	43.8
Region4/M804	47.6	41.9	46.6	43.3
Region6/MPL6	47.5	38.8	45.7	40.6
Region18/M318	47.5	42.1	46.3	43.4
Region20/M020	47.6	41.9	46.6	43.5
Region22/M022	47.7	42.1	46.4	43.6

According to the average values reported above, the worst signal to noise ratio belongs to the reference station that is located in the sixth district of the city (MPL6). Figure 7 illustrates the corresponding details both for GPS and GLONASS satellites observed from this station.

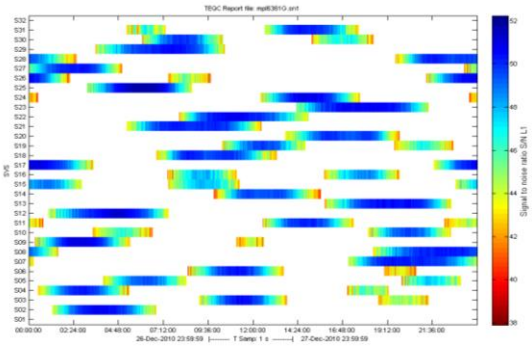

(a) L1

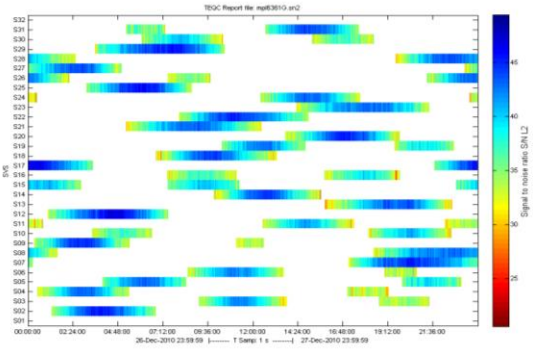

(b) L2

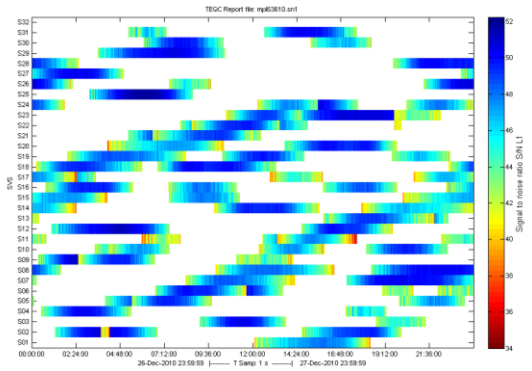

(c) L1

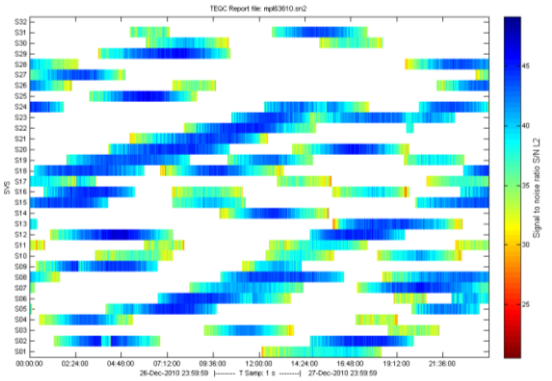

(d) L2

Fig. 7: Signal to noise ratio computed for (a &b) GPS and (c & d) GLONASS positioning signals received at station MPL6

3.2.5. Cycle slip

Every temporary disconnection of carrier signal or cycle slip leads to emerging a new unknown parameter (ambiguity) to the observation equation and therefore reduces the degree of freedom. This can result in restricted accuracies for the position of both reference and rover receivers. Appropriate site selection decreases the possibility of cycle slip on carrier phase measurements. As the result, the number of cycle slips for each station has been computed using both GPS and GLONASS observations. Table 6 represents the obtained results.

Table 6: Cycle slips on the GNSS observations of reference stations of TNRTK

	Cycle slip on GPS signal		Cycle slip on GLONASS signal	
Marker Name/Number	Number	Percentage	Number	Percentage
Region1/M501	171	0.023	49	0.010
Region4/M804	94	0.012	65	0.013
Region6/MPL6	49	0.006	58	0.012
Region18/M318	49	0.006	58	0.012
Region20/M020	145	0.019	46	0.009
Region22/M022	153	0.021	60	0.013

The seldom ratio of cycle slips to the total amount of observations acknowledges the site selection process.

3.3. Evaluation of special measures

3.3.1. Spatial variation of TEC

The Global Ionosphere Models (GIMs) are not constrained with the GPS data measured in the Iranian Permanent GPS Network (IPGN). Moreover, the spatial resolution of GIMs is larger than size of the city of Tehran.

Therefore, to decide on the impact of the refraction of the GNSS signals in Ionosphere on the network size estimating a local ionosphere model is more than just a desirable choice. In this project, to estimate a local TEC model Bernese v5.0 software has been utilized. In this software, the local TEC model is represented by (Dach et al. 2007):

$$TEC(\beta,s)=\sum_{n=0}^{n_{\max}}\sum_{m=0}^{m_{\max}}E_{nm}\left(\beta-\beta_0\right)^n\left(s-s_0\right)^m \qquad (5)$$

Where $n_{\max}$ and $m_{\max}$ are the maximum degree and order of the two dimensional Taylor series expansion of TEC in latitude β and longitude s. The coefficients E_{nm} are the unknown coefficients in the Taylor series which are to be estimated and β_0, s_0 are the coordinates of the origin of development. The parameter β is the geographical latitude and the parameter s is the sun-fixed longitude of the ionospheric pierce point. The noticeable point is that to map TEC, the so-called geometry-free linear combination of phase observations, which in principal contains ionospheric information, is analyzed. Figure 8 represents the spatial distribution of TEC within the expected territory of the TNRTK.

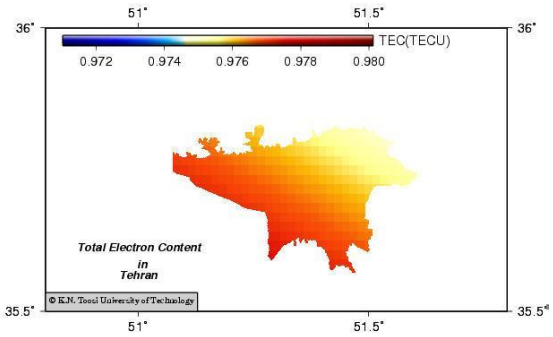

Fig. 8: The local TEC model computed from the GNSS data of the TNRTK.

According to this model, the electron density varies between $0.975 TECU$ and $0.978 TECU$ For observations with the maximum zenith angle of 70 degrees, this amount of variation in TEC results in the scale error below:

$$\frac{\Delta l}{l}=-0.7\times10^{-17}\times0.003\times10^{16}=-0.00021\,ppm \qquad (6)$$

As was anticipated at the design step, this amount of error does not play a remarkable role in selecting the position of the reference stations in the Tehran RTK network.

3.3.2. Tropospheric variation

Sensitivity analysis of the Saastamoninen's dry path delay together with the analysis of the synoptic meteorological stations next to the city of Tehran in section 2-2-3 suggested the optimum design for TNRTK. However, the synoptic stations of this study do not coincide with the network stations located next to the territory of the city, e.g. the western and eastern stations have relatively large distances with the corresponding reference stations in the TNRTK. Therefore, devising an independent verification method seems to be justifiable. The comparison of tropospheric Zenith Path Delays (ZPD) between the network stations is a reasonable methodology for this purpose: significant differences between ZPD at northernmost and southernmost stations as well as the most eastern and the most western points of the network is a quantitative measure to check remarkable changes in the corresponding meteorological conditions.

Precise Point Positioning (PPP) is used for estimating ZPDs at the position of the network stations. The PPP software of the Canadian Natural Resources (NRCan) has been utilized for this purpose. This software implements Least-squares weighted adjustment in order to estimate the unknown parameters, including the initial phase ambiguities, station coordinates and ZPDs. Therefore, estimated unknowns are gradually improved. Moreover, the unfavorable geometry of positioning at the first epochs makes the first parameter estimations unreliable. This can be seen in Figure 9.

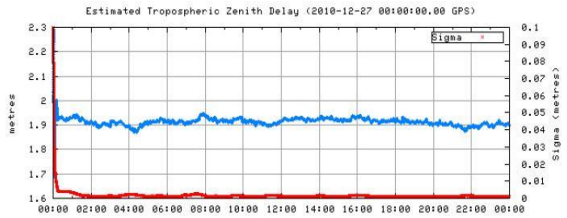

Fig. 9: ZPD estimation for the reference station M01

The difference between the ZPD of the most northern point (M501) and the most southern point of the network (M020) as well as the corresponding amount for stations located at the most western and most eastern part of the network (stations M022 and M804 respectively) have been estimated and

visualized in Figure 10. The mean differences of ZPD for west-east and north-south directed baselines are 16.3 cm and 2.2 cm respectively. This amount of difference between stations M501 and M020 confirms the speculations which are based on meteorological data of synoptic stations in the step of design. In fact, assuming a linear trend for the gradient of ZPD between the northern and southern parts of the city, ZPD gradient in this direction is $0.63 ppm$. Based on this gradient, the ZPD difference between the most northern point of the first proposed design and the northernmost point of the city would be more than 5 cm which is not satisfying the expected accuracy of an NRTK.

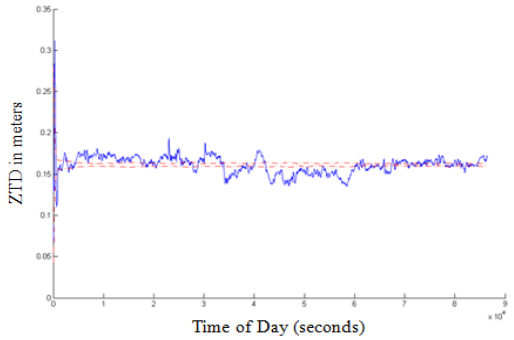

(a)

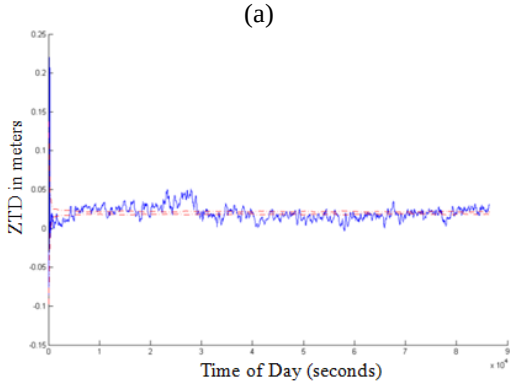

(b)

Fig. 10: Differences in ZPD estimates at the bounding stations a) M501 versus M020 & b) M804 versus M022

4. Testing the TNRTK

Checking the efficiency of the chosen design is the last step in comprehensive realization of the TNRTK. In an efficient RTK network, coordinates of the roving receiver are repeatable and determined within the precision and accuracy limits defined in the design process. In this paper, two different approaches have been used for checking the efficiency of the TNRTK. Both of the adopted approaches mathematically employ statistical testing of the samples.

In the first approach a set of points within the city of Tehran have been chosen and their positions are determined independently using kinematic as well as static positioning techniques. Different correction estimation and dissemination algorithms have been applied for kinematic positioning of the test points. These include Flächen Korrektur Paramter (FKP) (German phrase for spatial correction parameters), Master Auxiliary Concept (MAX) and individual Master Auxiliary Correction (i-MAX) techniques (Jazwinski, 1970, Euler et al. 2001). The distribution of these points is depicted in Figure 11. The green points in this figure illustrate the test points that are used in practice, while the blue points are the proposed test points. Coordinates determined by the application of different correction estimation and transmission algorithms are usually assigned different quality factors by the roving receiver. Therefore, the test grid provides a weighted sample for analyzing the TNRTK. The samples' size in this approach depends on the number of consecutive measurements at every point of the test gird. To reduce the execution cost of this phase of the project, the municipality has unfortunately limited the sample sizes to three.

The small samples generated for testing the TNRTK in the first approach prohibits a reliable evaluation of the efficiency of this NRTK. This fact makes the demand of the application of a second approach inevitable. In the second approach, one of the reference stations virtually plays the role of a rover receiver (test point) while it is not contributing in computing the network corrections. In other words, the number of reference stations of the network reduces to five. To check the efficiency of the TNRTK within the network area, the central point of the network (point MPL6) has been considered as the test point. Subsequently, to investigate the efficiency of the TNRTK for the points outside the network area, the reference station located at the most northern part (M501) has been considered as the test point in this process. VRS is the applied algorithm for the estimation and transmission of the corrections in this approach. Kinematic positioning of the test point in this approach is based on kinematic processing of the input data, while the measurements are originally made in static mode. Each time, the kinematic positions of the test point have been estimated in 7 different

batches of 1 hour length. The sampling rate of measurements in every batch is 30 seconds and kinematic positions are estimated in each epoch. In contrary to the first approach, because of using a single algorithm for estimating the corrections in this approach (VRS), kinematic coordinates of the test point provides a simple sample for further analysis.

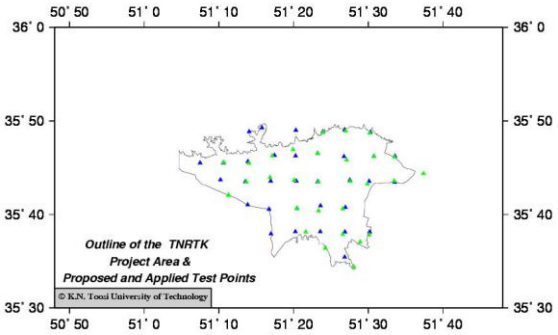

Fig. 11: distribution of the test points of first approach within the Tehran city

In the following subsections the concepts and corresponding results for precision, accuracy and repeatability of the test points' coordinates are given in further detail.

4.1. Repeatability

Repeatability of the kinematic coordinates is one of the suggested measures for checking the efficiency of a real time kinematic network. The measure is practically analyzed using the empirical Probability Density Function (PDF) of the obtained kinematic coordinates. Assuming that the coordinate errors in every sample of the kinematic coordinate is normally distributed, empirical PDFs of the kinematic coordinate components are expected to follow normal distributions whose means and variances are the static coordinates and sample variances. Optimistic estimation of the coordinate variances in static mode justifies the application of sample variances here. Therefore, the null and alternative hypotheses in this two-tailed test are as follows:

$$\begin{cases} H_0 : l_i \in N\left(\mu, s^2\right), & \alpha ; \forall i = 1,...,N \\ H_1 : l_i \notin N\left(\mu, s^2\right) \end{cases} \tag{7}$$

In this equation: elements $l_i \in \mathbf{l} = \left[l_1, l_2, ..., l_N\right]^T$ are either of the kinematic Cartesian coordinates of the test stations (for example the x component). Furthermore, μ and σ are the population mean and variance respectively. Finally, α is known as the significance level of the test. This parameters is the probability of rejecting the null hypothesis when it is, in fact, true (the so called type I error in hypothesis testing). Further theoretical details can be seen for example in (Teunissen, 2000a).

- **First approach**

Checking repeatability using the method outlined above requires a sample of sufficient size (e.g. more than 50 elements). Since the samples' sizes in this approach do not satisfy this condition, the analysis of the repeatability of the kinematic coordinates is not possible using the coordinate sample of the test grid in this approach.

- **Second approach**

In contrary to the previous approach, the hypothesis test for normality can be conducted in this approach. A confidence level of 95% has been considered for this purpose. Using the simple sample of coordinates in this approach, the unbiased estimate for the RMS of the coordinate components, for example x, is computed using (Teunissen, 2000b):

$$s_x = \left[\frac{\sum_{j=1}^{N} \left(x_{j,k}^{RTK} - x_k^{static} \right)}{N} \right]^{\frac{1}{2}} \tag{8}$$

In which x_k^{static} is the x-component of the static coordinate of the test point k and N is the number of components in the sample. Table 8 summarizes the obtained results in process of testing the TNRTK. Test points are introduced in the first column of this table. The second column of the table lists the time intervals or batches that the original static measurements have been broken to. The fifth column of the table reports on the results of the test for normality of the kinematic coordinates. The abbreviations P and F explain the result of the hypothesis tests. P is used for a hypothesis test which is passed and F indicates that the null hypothesis has been rejected. For the sake of brevity, Figure 12 visually compares the empirical PDFs obtained from one of the samples (for both of the test stations in this approach) to the corresponding population probability density functions. As it can be seen

in the Table 8, null hypothesis for normality test is passed for all the samples. This shows that the kinematic positions obtained using TNRTK base stations are repeatable. It is noticeable that, based on Eq. (8), the amount of bias directly influences the amount of RMS. Thereof, when the amount of bias is unacceptably large, to come up with an idea about the dispersion of the samples the RMS can be calculates using (Teunissen, 2000b):

$$\sigma_x = \left[\frac{\sum_{j=1}^{N} \left(x_{j,k}^{RTK} - \bar{x}_k^{RTK} \right)}{N-1} \right]^{\frac{1}{2}} \tag{9}$$

In which $\bar{x}_k^{RTK}$ is mean of the kinematic coordinate components which will be discussed in the next subsection. Therefore, RMSs of the samples containing the z-components of kinematic coordinates at M501 station are calculated using Eq. (9). Using this estimate of RMSs for these samples the null hypothesis of normality test has been passed.

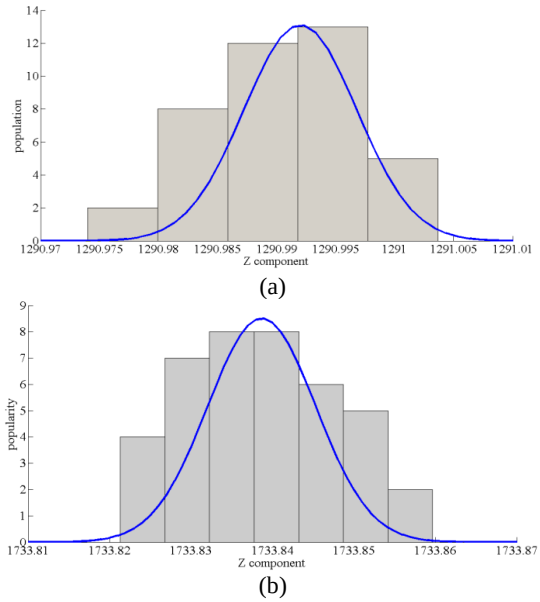

(a)

(b)

Fig. 12: Empirical PDF of the sample and corresponding population probability density function: a) z component of the kinematic coordinate of MPL6 in the time interval of 15:00 to 16:00, b) z component of the kinematic coordinate of M501 in the time interval of 15:00 to 16:00

4.2. Accuracy analysis of the kinematic coordinates

Investigating the accuracy of kinematic coordinates for a roving receiver stipulates its comparison to the position obtained through a method which is independent of the bias sources that influences the real-time coordinates. Here, the static positions are the only choice for this purpose.

The test of hypothesis for the population mean is a statistical measure for deciding on the presence of any bias in a sample. Assuming that the sample is drawn from a normal population, the hypothesis of this statistical test is as follows:

$$\begin{cases} H_0 : \mu = \bar{l}, & \alpha \\ H_1 : \mu \neq \bar{l} \end{cases} \tag{10}$$

In which $\bar{l}$ and μ are the sample and population means respectively. The static coordinates of the test points are taken as the population mean in this study. Moreover, the sample standard deviations are preferred again to the standard deviations of the static coordinates. Further theoretical detail is given for example in (Teunissen, 2000a). The hypothesis test for mean has been applied to the samples obtained in both approaches of this research. Probability of the type I error has been considered to be 5% again.

- **First approach**

The sample mean $\bar{l}$ is computed using weighted mean of the kinematic coordinate components using equation below (Teunissen, 2000b):

$$\bar{x}_k^{RTK} = \frac{\sum_{j=1}^{N} w_j x_{j,k}^{RTK}}{\sum_{j=1}^{N} w_j} \tag{11}$$

In this equation, index k refers to the desired test point and N is the corresponding sample size. The null hypothesis is passed for all points of the test grid. Nevertheless, the small samples' size reduces the reliability of the obtained results.

- **Second approach**

The sample mean $\bar{l}$ is computed using the simple sample of the kinematic coordinates using the equation below (Teunissen, 2000b):

$$\bar{x}_k^{RTK} = \frac{\sum_{j=1}^{N} x_{j,k}^{RTK}}{N} \tag{12}$$

The index k here refers to the either of test points MPL6 or M501. To report on the obtained results, abbreviations similar to the repeatability analysis are used here again. The sixth column of Table 8 provides the corresponding results. On the other hand, to come up with an estimate for the bias in the coordinate components of every batch (for example, x), computed kinematic coordinate in each component are averaged using Eq. (12) and then are extracted from its static counterpart $\left(\Delta x = x_k^{static} - \bar{x}_k^{RTK}\right)$. Third column of Table 8 provides the obtained results.

The null hypothesis for the samples of the z-component obtained in the time intervals of 11:00 to 12:00 and 21:00 to 22:00 are rejected for the test point MPL6. However, according to the three-sigma rule, the difference between the majority of the sample elements and the corresponding static coordinate is less than the expected accuracy limit which has been already defined for the TNRTK (3 cm). Figure 13 tries to clarify this point in further detail: According to this figure, for the sample obtained at noon, the bias of only 4.4% ($2*2.09 \approx 4.2mm$) of the z-components is more than this threshold. This fact can also be easily extended to the other sample mentioned above. In this case, the number of sample elements whose bias is larger than this threshold reduces to 0.2% ($3*9.6 \approx 2.9mm$). This is because the RMS of this sample is smaller than the RMS of the first one.

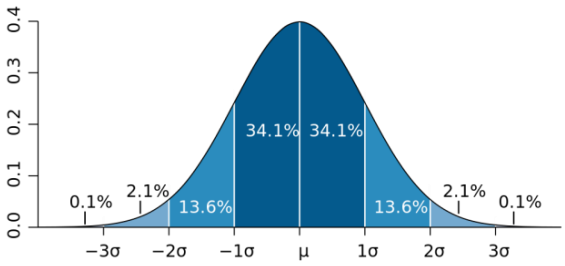

Fig. 13: three- sigma or empirical rule

For the test point M501 (the outside point), the null hypotheses for almost half of the samples of the y-components and all the samples of the z-components are rejected. The samples' root mean square errors for the y kinematic coordinates at this point are less than the corresponding samples' root mean square errors for station MPL6. Therefore, the rejection of the null hypotheses for the y-kinematic coordinates at this station can be justified by the same logic as stated for station MPL6. The big size of biases in the z-components of the northernmost part of Tehran was expected following the ZPD differences reported in section 3-3-2. The failure of the mean test for the z-components of station M501 confirms the applied strategy for selecting the second design as the optimum one. It is emphasized here again that station M501 is used as the test point and its measurements did not contribute in the process of producing network corrections.

4.3. Precision analysis of the kinematic coordinates

Dispersion of a random quantity is a measure for its precision and can be represented through its RMS error. Therefore the RMS of the test points has been calculated as a measure for the attainable precision in TNRTK.

- **First approach**

Using the small weighted sample of the coordinate components in this approach, the unbiased estimate of the RMS for the coordinate components, for example x, is given by (Teunissen, 2000b):

$$s_{x_k} = \left[\frac{\sum_{j=1}^{N} w_j}{\left(\sum_{j=1}^{N} w_j\right)^2 - \sum_{j=1}^{N} w_j^{\,2}} \sum_{j=1}^{N} w_j \left(x_{j,k}^{RTK} - \bar{x}_k^{RTK} \right)^2 \right]^{\frac{1}{2}} \qquad (13)$$

In this equation $\bar{x}_{j,k}^{RTK}$ is the weighted average of the sample which corresponds to the test point k and can be calculated using Eq. (11). Table 7 represents the obtained results.

Based on the results shown in this table, only four of the stations have an unacceptable amount of RMS. This may be due to the inconsistency of corrections transmitted using different algorithms in a particular situation or mistakes in measurement process.

Table 7: weighted RMS calculated for the kinematic positions of the test points

No.	Test station name	σ_x cm	σ_Y cm	σ_z cm	No.	Test station name	σ_x cm	σ_Y cm	σ_z cm
1	T01-1	0.47	0.31	0.15	17	T11-1	0.25	0.12	0.23
2	T01-2	0.28	0.08	0.2	18	T12-1	0.88	0.08	0.36
3	T02-1	0.35	0.04	0.01	19	T15-1	0.77	0.28	0.23
4	T02-2	0.12	0.08	0.11	20	T15-2	0.14	0.26	0.11
5	T03-1	0.64	0.24	0.13	21	T15-3	0.72	0.13	0.1
6	T04-1	1.04	0.16	0.08	22	T18-1	0.35	0.14	0.55
7	T04-2	1.28	0.09	0.08	23	T19-1	0	0.06	0.05
8	T04-3	3.78	3.51	1.98	24	T20-1	0.78	0.04	0.09
9	T05-1	0.8	0.08	0.1	25	T20-2	1.2	0.15	0.23
10	T05-2	1.41	0.2	0.26	26	T21-2	0.21	0.05	0.14
11	T07-1	0.41	0.11	0.21	27	T21-3	0.71	0.23	0.46
12	T08-1	1.21	0.07	0.08	28	T21-5	4.38	0.63	2.72
13	T08-2	1.06	0.07	0.38	29	T22-2	1.27	0.08	0.24
14	T09-1	0.11	0.14	0.02	30	T22-3	0.57	0.04	0.56
15	T09-5	2.69	0.26	0.27	31	T22-6	8.1	4.14	9.69
16	T09-5	2.69	0.26	0.27	32	T22-7	0.07	2.24	6.35

- **Second approach**

Using the simple sample of the coordinate components in this approach, the unbiased estimate of the RMS of the coordinate components, for example x, is computed using Eq. (8). The forth column of Table 8 reports the obtained results. As it is mentioned in section 4-1, RMSs of the samples containing the z-components of the kinematic coordinates of station M501 are calculated using Eq. (9) due to large amount of bias in these components compared to corresponding static component.

Table 8: Results of hypothesis test for normality and mean as well as the amount of biases and variances of the samples

Test point	Batch interval (start -end)	Bias (mm)			RMS (mm)			Result of the normality test			Result of the mean test		
		Δx	Δy	Δz	σ_x	σ_y	σ_z	x	y	z	x	y	z
Center (MPL6)	3 – 4	-0.2	-1.6	-1.05	2.0	2.9	6.9	P	P	P	P	P	P
	6 – 7	-0.8	-0.9	8.1	4.6	4.7	19.3	P	P	P	P	P	P
	9 – 10	0.1	1.1	2.8	1.9	4.0	6.8	P	P	P	P	P	P
	11 – 12	-0.3	2.3	9.6	3.2	6.3	20.9	P	P	P	P	P	F
	15 – 16	1.2	0.5	-1.6	2.2	2.8	6.8	P	P	P	P	P	P
	18 – 19	0.28	-0.5	4.3	4.3	1.4	7.0	P	P	P	P	P	P
	21 – 22	0.5	1.1	7.3	1.6	2.8	9.6	P	P	P	P	P	F
North (M01)	3 – 4	2.1	3.2	72.7	3.4	4.7	9.3	P	P	P	P	P	F
	6 – 7	2.2	3.7	72.8	6.2	6.1	16.0	P	P	P	P	F	F
	9 – 10	0	0.06	81.2	2.5	6.3	9.6	P	P	P	P	P	F
	11 – 12	-1.7	5.9	60.8	7.4	11.6	27.8	P	P	P	P	F	F
	15 – 16	1.1	3.9	70.2	3.4	5.6	9.1	P	P	P	P	F	F
	18 – 19	0.7	1.6	64.2	3.1	5.2	8.3	P	P	P	P	P	F
	21 – 22	1.4	5.4	67.0	3.6	6.8	11.1	P	P	P	P	F	F

5. Conclusion

This paper discusses on three consecutive steps in comprehensive implementing of an RTK network in the city of Tehran. These include investigation of different measures for designing the TNRTK and locating its reference stations, verifying the design measures and finally testing the efficiency of this NRTK. The main aim of the first step was to select the optimum design among two proposed configurations for this NRTK. The proposed designs were based on two different considerations: increasing the common visibility of the GNSS satellites which can be obtained by decreasing the extent of the RTK network, and decreasing the impact of distance-dependent errors which leads to increasing the extent of this NRTK. General measures including visibility of satellites, geometry of positioning, and elevation angle of the satellites to be tracked as well as noise of measurement and the success rate in resolving the ambiguity of carrier phases have been analyzed. Additionally, special measures (distance dependent errors) including: orbital

error, variation of electron density in ionosphere and tropospheric variation are also analyzed for the two proposed designs. It is seen that the tropospheric variation is the most prominent measure among the others and that it suggests the second design as an optimum one for the TNRTK.

In the second step, 24 hour of simultaneous code and carrier phase observations of the reference stations of the optimum design selected in the first step have been used to check the measures involved in choosing the optimum design. Therefore, the difference between this and the first step is the methodology of processing. It means that, in this step all the measures are investigated using real GNSS measurements. However, the results of this step show a complete consistency with the corresponding results in the design level. This results in the anticipation of obtaining the presupposed accuracy and precision of an NRTK using the Tehran RTK network.

The last step is testing the efficiency of the TNRTK using the test measurement campaigns. As the first approach for this purpose, a set of points within the Tehran city have been chosen and their positions are determined independently using kinematic as well as static positioning techniques. However, due to small sample sizes a second approach has been also devised. In this approach, one of the reference stations virtually plays the role of a rover receiver (test point) while it is not contributing in computing the network corrections. This method has been applied for the central and northern reference stations of the TNRTK. Precision, accuracy and repeatability of the test points' coordinate are analyzed using mathematical statistics. The results of these analysis show that the TNRTK completely fulfills the promised efficiency of an NRTK within the territory of Tehran city.

6. Acknowledgment

We would like to appreciate the Geobite Company for their cooperation in this project. Also we would like to appreciate them for providing the chance of using a licensed version of the Bernese version 5.0 in this project.

References

[1] Bauersıma I (1983) NAVSTAR/Global Positioning System (GPS), II., Mitteilungen der Satelliten-Beobachtungsstation Zimmerwald, No. 10, Astronomical Institute, University of Berne.

[2] Beutler G, Bauersima I, Gurtner W, Rothacher M, Schildknecht T, Geiger A (1988) Atmospheric refraction and other important biases in GPS carrier phase observations. In: Atmospheric effects on geodetic space measurements, Monograph 12, School of surveying, University of New South Wales, Australia, pp 15–43.

[3] Blewitt G. (1998) GPS data processing methodology: from theory to applications. GPS for Geodesy, pp 231-270. Springer-Verlag, Berling.

[4] Chen XM, Han SW, Rizos C, Goh PC (2000) Improving real time positioning efficiency using the Singapore Integrated Multiple Reference Station Network (SIMRSN). In: Proceeding of the 13th International Technical Meeting of the Satellite Division of the US Institute of Navigation, Salk Lake City, UT, September 19-22, pp 9-16.

[5] Dach R, Hugentobler U, Fridez P, Meindl M (2007) Bernese GPS software version 5.0. Astronomical Institute, University of Bern.

[6] Dai L, Han S, Wang J, Rizos C (2001) A study on GPS/GLONASS multiple reference station techniques for precise real-time carrier phase-based positioning. In: proceedings of ION GPS 2001, pp 392-403.

[7] El-Mowafy A, Fashir H, Al Marzooqi Y, Al Habbai A, Babiker T (2003) Testing of the DVRS national GPS-RTK network. In: Proceedings of the 8th ISU International Symposium, Strasbourg, France, May 25–28.

[8] Estry L, Meertens CM (1999), TEQC: the multi-purpose toolkit for GPS/GLONASS data. GPS Solut, 3(1):42–49.

[9] Euler HJ, Keenan CR, Zebhauser BE, Wubenna G (2001) Study of a simplified approach in utilizing information from permanent reference station arrays. In: Proceeding of ION GPS 2001, Salt Lake City, 11–14 September, pp 379–391.

[10] Feltense J (1998) Chapman profile approach for 3-d global TEC representation. In: Proceeding of the IGS Analysis Center Workshop, ESOC, Darmshtadt, Germany, February 9–11, pp 285–297.

[11] Gordini C, Kealy AN, Grgich PM, Hale MJ (2006) Testing and evaluating of a GPS CORS network for real–time centimetric positioning – The Victoria GPSnet™. In: Proceeding of the IGNSS2006 Symposium, 17-21 July, Gold Coast, Australia.

[12] Hakli P (2004) Practical test on accuracy and usability of Virtual Reference Station method in Finland, FIG Working Week 2004, Athens, Greece, May 22-27.

[13] Janssen V (2009) A comparison of the VRS and MAC principles for network RTK. International Global Navigation Satellite Systems Society, IGNSS Symposium, Holiday Inn Surfers Paradise, Qld, Australia, December 1–3.

[14] Jazwinski AH (1970) Stochastic process and filtering theory. Academic Press.

[15] Han S (1997) Carrier phase-based long-range GPS kinematic positioning. PhD Thesis, School of Surveying and Spatial Information Systems, University of New South Wales, Sydney, Australia.

[16] Klobuchar JA, (1987) Ionospheric time-delay algorithm for single-frequency GPS users. IEEE Trans. on Aerospace and Electronic Systems, AES-23(3), pp 325–331.

[17] Landau H, Vollath U, Chen X (2003) Virtual reference station versus broadcast solutions in network RTK – advantages and limitations. In: Proceedings of GNSS 2003 – The European Navigation Conference, Graz, Austria, April 22-25, 2003.

[18] Leick A (1994) GPS satellite surveying. 2nd Edition, John Wiley & sons, 1994, USA.

[19] Marel H (1998) Virtual Reference Stations in the Netherlands. In: Proceedings of ION GPS 1998, 15-18 September, Nashville, Tennessee, USA, pp 49-58.

[20] Mehrabadi KM (2012) Design of satellite geodetic networks. Department of Geodesy, Faculty of Geodesy and Geomatics Engineering, Tehran. K. N. Toosi University of Technology, Msc. Thesis.

[21] Ogaja C, Hedfors J (2007) TEQC multipath metrics in Matlab. GPS Solut 11(3): 215-222.

[22] Petrovski I, Kawaguchi S, Torimoto H, Townsend B, Hatsumoto S, Fuji K (2002) An impact of high ionospheric activity on MultiRef RTK network performance in Japan. In: Proceedings of the 15th International Technical Meeting of the Satellite Division of the Institute of Navigation (ION GPS 2002), Portland, OR, September 2002, pp 2247–2255.

[23] Rizos C (2003) Network RTK research and implementation – A geodetic perspective. Journal of Global Positioning Systems, 1(2):144–150.

[24] Rizos C, Yan TS (2004) Development of SydNet permanent real–time GPS network. Journal of Global Positioning Systems, 3(1–2), pp 296-301.

[25] Schaer S, Beutler G, Mervart L, Rothacher M, Wild U (1995), Global and regional ionosphere models using the GPS double difference phase observable. IGS Workshop, Proceedings on special topics and new directions, GeoForschungsZentrum, Postdam, pp 77–92.

[26] Seeber G (2003) Satellite Geodesy. 2nd completely revised and extended edition, Walter de Gruyter, ISBN 3-11-017549-5.

[27] Smith WHF, Wessel P (1990) Gridding with continuous curvature splines in tension. Geophysics, 55: 293-305.

[28] Treinish LA, Gough ML (1987) A software package for the data-independent management of multidimensional data EOS, 68: 633-635.

[29] Teunissen PJG (2000a) Testing Theory; an Introduction. Delft University Press, Delft, 1st edition.

[30] Teunissen PJG (2000b) Adjustment Theory; an Introduction. Delft University Press, Delft, 1st edition.

[31] Vollath U, Landau H, Chen X (2002) Network RTK – concept and performance. In: Proceedings of the GNSS Symposium, Wuhan, China.

[32] Wild U, Beutler G, Gurtner W, Rothacher M (1989) Estimating the ionosphere using one or more dual frequency GPS receivers. In: Proceedings of the 5th International Geodetic Symposium on satellite positioning, Las Cruces, New Mexico, Vol. 2, pp. 724-736, March 13-17.

[33] Wubbena G, Bagge A, Seeber G, Boder V, Hankemeier P (1996) Reducing distance dependent errors for real–time precise DGPS applications by establishing reference station networks. In: Proceedings ION GPS 96, Kansas City, Missouri, pp 1845–1852.

[34] Zielinski JB (1988) Covariance in 3D Networks Resulting from Orbital Errors. In: Lecture Notes in Earth Sciences, GPS-Techniques applied to Geodesy and Surveying, pp. 504–514, Springer-Verlag, Berlin.